Supplementary Materials to

Bradyrhizobium ivorense sp. nov. as a potential local bioinoculant for *Cajanus cajan* cultures in Côte d'Ivoire

by **Romain K. Fossou, Joël F. Pothier, Adolphe Zézé and Xavier Perret***

* Corresponding author: xavier.perret@unige.ch

Table S1. Origin of the *C. cajan* nodule isolates proposed as *B. ivorense* sp. nov. strains.

Table S2. List of primers and sequences of *C. cajan* nodule isolates used in this study.

Table S3A. Names and corresponding GenBank accessions for eight type strains selected to represent the *B. japonicum* super clade.

Table S3B. Names and corresponding GenBank accessions for the 21 type strains of the *B. elkanii* supergroup that were used for phylogenetic analyses.

Table S4. Levels of similarity between concatenated *dnaK-glnII-gyrB-recA-rpoB* sequences of bradyrhizobia.

Table S5. Overview and general characteristics of the CI-1B^T and CI-41S genomes.

Table S6. Phenotypic characteristics of *B. ivorense* sp. nov. strains and *B. elkanii* USDA 76^T.

Table S7. Symbiotic phenotype of selected *B. ivorense* sp. nov. isolates on diverse legumes.

Figure S1. Maximum likelihood phylogram inferred from partial 16S rRNA gene sequences.

Figure S2. Maximum likelihood phylogram inferred from partial *dnaK* gene sequences.

Figure S3. Maximum likelihood phylogram inferred from partial *glnII* gene sequences.

Figure S4. Maximum likelihood phylogram inferred from partial *gyrB* gene sequences.

Figure S5. Maximum likelihood phylogram inferred from partial *recA* gene sequences.

Figure S6. Maximum likelihood phylogram inferred from partial *rpoB* gene sequences.

Figure S7. Maximum likelihood phylogram inferred from concatenated partial *glnII* and *recA* gene sequences

Figure S8. Maximum likelihood phylogram inferred from partial *nifH* gene sequences.

Table S1. Origin of the *C. cajan* nodule isolates proposed as *B. ivorense* sp. nov. strains.

	Strain	Plant #	Field # (GPS coordinates)	Locality
1.	**CI-1B^{T} ***	1	1 (N 7°17′45″ - W 5°49′00″)	Kossou-Bouafla
	CI-4A2	4		
	CI-4A3			
	CI-4C			
5.	CI-4D			
	CI-14A	14	3 (N 6°51′19″ - W 5°14′38″)	Yamoussoukro
	CI-14B			
	CI-15A	15		
	CI-15D			
10.	CI-18C	18	4 (N 6°51′02″ - W 5°13′31″)	
	CI-19A1	19		
	CI-19D			
	CI-19E			
	CI-33F	33	5 (N 7°55′28″ - W 2°57′45″)	Bondoukou
15.	CI-33K			
	CI-35B	35		
	CI-41B	41	6 (N 7°56′50″ - W 2°56′26″)	
	CI-41L			
19.	**CI-41S ***			

Legend to Table S1. Nodule isolates that were sequenced for multilocus sequence analyses (MLSA) are shown in bold and those for which genome data was collected are marked by an asterisk. Strains that are underlined were tested for nodulation and symbiotic nitrogen-fixation on *C. cajan* cvs. ILRI 16555 and “Light Brown”. Strains in bold were also inoculated onto *Glycine max* cv. Davis, *Macroptilium atropurpureum* cv. Siratro, *Leucaena leucocephala*, *Tephrosia vogelii*, *Vigna radiata* cv. King and *Vigna unguiculata* cv. Red Caloona, and the phenotypes on these host plants can be found in Table S7.

Table S2. List of primers and sequences of *C. cajan* nodule isolates used in this study.

Primer	**5' to 3' sequence**	**Size** (bases)	**Amplicon** (bp)	**Reference**
dnaK-For	GGTGACCTTCGACATCGACG	20		this work
dnaK-Rev	CGGTGAACTCCGCGTCGAC	19	461	this work
glnII-For1	TGACCAAGTACAAGCTCGAGT	21		this work
glnII-Rev1	GAGAAGTTGGCGTGCATGCC	20	700	this work
gyrB-For1*	TTCGACCAGAACTCCTACAAGG	22		this work
gyrB-Rev1*	AGCTTGTCCTTGGTCTGCG	19	710	this work
recA-For	CAAGGGCTCGGTGATGAAGC	20		this work
recA-Rev	CGATGCGGCGGATGTCGAG	19	623	this work
rpoB-For	ACGGCACCGAGCGCGTCAT	19		this work
rpoB-Rev	GTCGTCGATCTCGCCCTTGC	20	923	this work

Strain	**Gene**	**Size** (bp)	**Accession**	**Reference**
CI-1B	16S-ITS-23S	2540	KX396570	Fossou et al. 2016
	dnaK	422	MK376326	this work
	glnII	659	MH756157	this work
	gyrB	669	MH756161	this work
	recA	584	MK376330	this work
	rpoB	923	KX388393	Fossou et al. 2016
CI-14A	16S-ITS-23S	2540	KX396573	Fossou et al. 2016
	dnaK	422	MK376327	this work
	glnII	659	MH756158	this work
	gyrB	669	MH756162	this work
	recA	584	MK376331	this work
	rpoB	884	MK376334	this work
CI-19D	16S-ITS-23S	2539	KX396575	Fossou et al. 2016
	dnaK	422	MK376328	this work
	glnII	659	MH756159	this work
	gyrB	669	MH756163	this work
	recA	584	MK376332	this work
	rpoB	884	MK376335	this work
CI-41S	16S-ITS-23S	2540	KX396584	Fossou et al. 2016
	dnaK	422	MK376329	this work
	glnII	659	MH756160	this work
	gyrB	669	MH756164	this work
	recA	584	MK376333	this work
	rpoB	884	MK376336	this work

Legend to Table S2. *GyrB-For1 and GyrB-Rev1 were derived from gyrB343F and gyrB1043R proposed by Martens et al. (2008).

Table S3A. List of the eight type strains and corresponding GenBank accessions used in this study as data for members of the *Bradyrhizobium japonicum* supergroup. The underlined accession includes one ambiguous (N) position.

			GenBank accession for corresponding gene					
	Type strain	Type strain genome data	16S rRNA	*dnaK*	*glnII*	*gyrB*	*recA*	*rpoB*
B. japonicum super clade	*B. arachidis* CCBAU 051107^{T}	NZ_FPBQ01000000	HM107167	JX437668	HM107251	JX437675	HM107233	JX437682
	B. betae LMG 21987^{T}	no genome available	AY372184	FM253303	AB353733	AB353735	AB353734	FM253260
	B. canariense BTA-1^{T}	no genome available	AJ558025	AY923047	AY386765	FM253220	AY591553	FM253263
	B. diazoefficiens USDA 110^{T}	NC_004463	gene sequences derived from archived genome data					
	B. iriomotense EK05^{T}	no genome available	AB300992	JF308944	AB300995	AB300997	AB300996	HQ587646
	B. japonicum USDA 6^{T}	NC_017249	gene sequences derived from archived genome data					
	B. liaoningense USDA 3622^{T}	no genome available	AF208513	FM253309	AY386775	FM253223	AY591564	EF190181
	B. ottawense OO99^{T}	CP029425	JN186270	JF308816	HQ587750	HQ873179	HQ587287	HQ587518

Table S3B. Type strains of the *B. elkanii* supergroup and corresponding sequences selected for phylogenetic analyses. Accessions that differ from genome data are shown in bold and those with ambiguous nucleotides (e.g. N, R or Y) are underlined. Note that *recA* of *B. ferriligni* CCBAU 51502^T (KJ818112) was identical to *recA* of *B. elkanii* CCBAU 05737 at both, genomic (NZ_AJPV00000000) and single gene accessions (HM057521).

			GenBank accession for corresponding gene					
	Type strain	Type strain genome data	16S rRNA	*dnaK*	*glnII*	*gyrB*	*recA*	*rpoB*
B. elkanii super clade	*B. algeriense* RST89^T	NZ_PYCM01000000	FJ546419	n.a.	**FJ264924**	n.a.	**FJ264927**	n.a.
	B. brasilense UFLA03-321^T	NZ_MPVQ01000000	**KF311068**	KF452791	n.a.	KF452827	KT793142	KF452879
	B. centrolobii BR 10245^T	NZ_LUUB01000000	**KF927049**	**KX527928**	KX527991	n.a.	**KX527954**	KF983827
	B. elkanii USDA 76^T	NZ_ARAG00000000	**HQ233240**	AM168363	AY599117	AB070584	AY591568	LC167350
	B. embrapense SEMIA 6208^T	NZ_LFIP00000000	**AY904773**	KP234519	GQ160500	HQ634891	HQ634899	**HQ634910**
	B. erythrophlei CCBAU 53325^T	no genome available	KF114645	MG811656	KF114693	KF114717	KF114669	MG811654
	B. ferriligni CCBAU 51502^T	no genome available	KX683400	MG811657	KJ818099	KJ818102	KJ818112	MG811655
	B. icense LMTR 13^T	CP016428	KF896156	KF896182	KF896175	KF896201	JX943615	n.a.
	B. jicamae PAC68^T	NZ_LLXZ01000000	**AY624134**	JN207408	FJ428204	HQ873309	HM590776	HQ587647
	B. lablabi CCBAU 23086^T	NZ_LLYB01000000	**GU433448**	KF962687	GU433498	JX437670	GU433522	JX437677
	B. macuxiense BR 10303^T	NZ_LNCU01000000	KX527919	KX527932	KX527995	KX528008	KX527958	KX527969
	B. mercantei SEMIA 6399^T	NZ_MKFI01000000	FJ025102	**KX690617**	KX690621	KX690623	**KX690615**	n.a.
	B. namibiense 5-10^T	no genome available	KX661401	KP402058	KM378440	KX661393	KM378377	KM378306
	B. neotropicale BR 10247^T	NZ_LSEF01000000	**KF927051**	KJ661693	KJ661700	KJ661707	**KJ661714**	KF983829
	B. pachyrhizi PAC48^T	NZ_LFIQ01000000	AY624135	JN207406	FJ428201	KF532651	HM047130	**LM994172**
	B. paxllaeri LMTR 21^T	NZ_MAXB01000000	AY923031	AY923038	KF896169	KF896195	JX943617	KP308154
	B. retamae Ro19^T	NZ_LLYA00000000	KC247085	LM994150	KC247108	KF962698	KC247094	LM994174
	B. ripae WR4^T	no genome available	MF593081	MF593102	MF593086	MF593094	MF593090	MF593098
	B. tropiciagri SEMIA 6148^T	NZ_LFLZ01000000	**AY904753**	**FJ391008**	FJ391048	HQ634890	**FJ391168**	**HQ634909**
	B. valentinum LmjM3^T	NZ_LLXX01000000	JX514883	n.a.	**JX518575**	n.a.	JX518589	n.a.
	B. viridifuturi SEMIA 690^T	NZ_LGTB01000000	FJ025107	**KR149128**	KR149131	KR149134	**KR149140**	KU724169

Table S4. Similarity levels between concatenated *dnaK-glnII-gyrB-recA-rpoB* (2,560 bp) sequences of bradyrhizobia. Strains were ordered by highest similarity to *B. ivorense* sp. nov strains CI-1B^T and CI-41S, except for *B. centrolobii* BR 10245^T (#22) and *B. neotropicale* BR 10247^T (#23) that better matched sequences of the *B. japonicum* super-clade representative strain USDA 6^T (#24) shaded in light grey. DNA sequences were from type strains *B. algeriense* RST89^T (#18), *B. brasilense* UFLA03-321^T (#7), *B. elkanii* USDA 76^T (#5), *B. embrapense* SEMIA 6208^T (#9), *B. erythrophlei* CCBAU 53325^T (#13), *B. ferriligni* CCBAU 51502^T (#12), *B. icense* LMTR 13^T (#17), *B. jicamae* PAC68^T (#16), *B. lablabi* CCBAU 23086^T (#14), *B. macuxiense* BR 10303^T (#11), *B. mercantei* SEMIA 6399^T (#10), *B. namibiense* 5-10^T (#19), *B. pachyrhizi* PAC48^T (#6), *B. paxllaeri* LMTR 21^T (#15), *B. retamae* Ro19^T (#20), *B. ripae* WR4^T (#4), *B. tropiciagri* SEMIA 6148^T (#3), *B. valentinum* LmjM3^T (#21) and *B. viridifuturi* SEMIA 690^T (#8). Values above the 97% threshold proposed by Durán et al. (2014) are underlined. Levels of the highest similarity to CI-1B^T and CI-41S are in bold.

	Strain	1	2	3	4	5	6	7	8	9	10	11	12	13	14	15	16	17	18	19	20	21	22	23
1	CI-1B^T	100			*B. ripae*	*B. elkanii*	*B. pachyrhizi*	*B. brasilense*	*B. viridifuturi*	*B. embrapense*	*B. mercantei*	*B. macuxiense*	*B. ferriligni*	*B. erythrophlei*	*B. lablabi*	*B. paxllaeri*	*B. jicamae*	*B. icense*	*B. algeriense*	*B. namibiense*	*B. retamae*	*B. valentinum*	*B. centrolobii*	*B. neotropicale*
2	CI-41S	98.4	100																					
3	*B. tropiciagri*	**95.2**	**95.3**	100																				
4	*B. ripae*	95.1	95.1	96.6	100																			
5	*B. elkanii*	95.1	95.0	96.6	96.7	100																		
6	*B. pachyrhizi*	95.1	94.9	96.8	96.6	97.8	100																	
7	*B. brasilense*	95.0	95.1	96.8	96.5	97.9	99.1	100																
8	*B. viridifuturi*	94.9	94.8	97.2	96.2	96.5	96.5	96.5	100															
9	*B. embrapense*	94.5	94.5	96.4	95.6	96.5	96.2	96.1	96.2	100														
10	*B. mercantei*	94.5	94.3	96.7	96.1	96.3	96.3	96.3	96.7	95.5	100													
11	*B. macuxiense*	94.4	94.6	94.8	94.3	95.6	95.3	95.2	94.6	94.6	94.6	100												
12	*B. ferriligni*	93.8	93.9	96.2	95.7	96.9	96.9	97.1	95.9	95.6	95.8	94.0	100											
13	*B. erythrophlei*	93.7	93.9	93.9	93.6	94.1	93.7	93.7	93.9	93.8	93.6	94.1	93.0	100										
14	*B. lablabi*	91.0	91.3	91.1	90.7	91.5	91.3	91.4	91.3	91.1	91.3	91.3	90.4	90.4	100									
15	*B. paxllaeri*	91.0	91.3	91.1	91.1	91.3	91.1	91.3	91.2	91.1	91.2	91.0	90.7	90.4	97.1	100								
16	*B. jicamae*	90.7	91.1	91.0	90.6	91.3	91.0	91.2	90.9	90.9	91.0	91.0	90.5	90.4	96.6	97.4	100							
17	*B. icense*	90.8	91.0	90.9	91.0	91.5	91.2	91.4	91.0	91.2	91.1	90.7	90.8	90.5	94.5	94.3	94.2	100						
18	*B. algeriense*	90.4	90.2	90.4	90.0	90.2	90.1	90.4	90.0	89.8	90.5	90.5	89.6	90.2	92.4	92.2	92.2	92.2	100					
19	*B. namibiense*	90.3	90.8	90.6	90.0	91.0	90.4	90.4	90.5	90.6	90.3	90.7	90.1	90.4	92.2	92.5	92.8	92.3	90.0	100				
20	*B. retamae*	90.1	90.4	90.7	90.4	90.9	90.7	91.1	90.5	90.8	90.7	90.3	90.1	89.8	94.0	93.6	93.7	95.4	91.6	91.0	100			
21	*B. valentinum*	89.8	89.9	89.9	89.6	90.0	89.5	89.8	89.6	89.7	89.9	90.0	89.5	89.9	91.9	91.8	91.9	92.2	94.8	90.3	91.1	100		
22	*B. centrolobii*	90.7	90.8	90.5	90.7	91.0	90.7	90.7	90.8	90.6	90.5	91.1	89.8	91.1	90.1	89.9	89.9	89.5	88.9	90.5	88.8	88.8	100	
23	*B. neotropicale*	90.5	90.9	90.4	90.2	90.3	90.0	90.1	90.1	90.2	89.9	90.6	89.3	90.5	89.7	89.4	89.6	88.9	88.5	90.2	88.2	88.4	95.7	100
24	*B. japonicum*	90.5	90.7	91.0	90.9	91.0	90.7	90.8	91.0	90.7	90.5	90.9	90.0	90.1	89.8	89.5	89.6	89.4	89.0	89.5	88.9	89.3	93.7	93.6

Table S5. Overview and general characteristics of the CI-1B^T and CI-41S draft genomes.

	CI-1B^T	**CI-41S**
Genome size (kb)	9,412	8,864
G+C content (mol%)	64.21	64.37
Number of contigs	44	59
Contig N_{50}	466,280	253,924
Contig L_{50}	4	11
Raw coverage	114.6 x	35.7 x
Number of predicted genes	8,546	8,123
Numbr of tRNAs	56	57

Table S6. Phenotypic characteristics of *B. ivorense* sp. nov. strains and *B. elkanii* USDA 76^T

Characteristic		**CI-1B^T**	**CI-14A**	**CI-19D**	**CI-41S**	**USDA 76^T**
Growth in liquid RMS at (°C)	20	+	+	+	+	+
	25	+	+	+	+	+
	27	+	+	+	+	+
	30	+	+	+	+	+
	35	–	–	w	w	+
	40	–	–	–	–	–
Growth in liquid RMS at pH	4 to 5	–	–	–	–	–
	6 to 8	+	+	+	+	+
	9 to 12	–	–	–	–	–
Growth in RMM with 20 (*10) mM	fructose	w	n.t.	n.t.	w	w
	galactose	+	n.t.	n.t.	+	+
	glucose	+	n.t.	n.t.	+	w
	malate*	+	n.t.	n.t.	+	+
	maltose	–	n.t.	n.t.	–	–
	mannose	w	n.t.	n.t.	w	+
	pyruvate	+	n.t.	n.t.	+	+
	succinate*	+	n.t.	n.t.	+	+
	sucrose	–	n.t.	n.t.	–	–
Growth in YM at 27°C with NaCl at	0.04%	+	+	+	+	+
	0.25%	+	+	+	+	+
	0.5%	+	+	–	w	+
	0.75%	–	–	–	–	w
	1.0%	–	–	–	–	–
Growth on RMS plates with (µg per antibiotic disc)	ampicilin (100)	+	+	w	–	–
	chloramphenicol (500)	+	+	+	+	+
	erythromycin (50)	+	+	+	+	+
	gentamycin (50)	+	+	+	+	+
	kanamycin (100)	+	+	+	+	–
	penicillin (10)	+	+	+	+	+
	streptomycin (250)	+	+	+	+	+
	tetracycline (50)	+	+	+	+	+
Reaction of (API 20NE)	fermentation	–	–	–	n.t.	–
	esculin hydrolysis	w	–	–	n.t.	–
	gelatin hydrolysis	–	–	–	n.t.	–
	arginine di-hydrolase	+	+	+	n.t.	+
	indole production	–	–	–	n.t.	–
	NO_3^- reduced to NO_2^-	–	–	–	n.t.	+
	NO_3^- reduced to N_2	–	–	–	n.t.	–
	urease	+	+	+	n.t.	+
	β-galactosidase (PNPG)	–	–	–	n.t.	–
Assimilation of (API 20NE)	adipic acid	+	+	+	n.t.	+
	capric acid	–	–	–	n.t.	–
	D-glucose	+	w	+	n.t.	w
	D-maltose	+	+	+	n.t.	w
	D-mannitol	+	+	+	n.t.	+
	D-mannose	+	+	+	n.t.	+
	L-arabinose	+	w	+	n.t.	w
	malic acid	w	w	w	n.t.	w
	N-acetylglucosamine	+	+	+	n.t.	w
	phenylacetic acid	w	w	w	n.t.	w
	potassium gluconate	+	+	+	n.t.	+
	trisodium citrate	w	w	w	n.t.	w

Legend to Table S6. +, positive for; –, negative for; w, weak for; n.t., not tested. For details on growth and resistance to antiobiotics, see main text. All strains were negative for catalase and positive for oxidase reactions.

Table S7. Symbiotic phenotype of selected *B. ivorense* sp. nov. isolates on diverse legumes.

	Host plant						
Inoculant	Cc (42 dpi)	Gm (49 dpi)	Ma (42 dpi)	Ll (98 dpi)	Tv (42 dpi)	Vr (35 dpi)	Vu (35 dpi)
CI-1B^T	Nod+ / Fix+	Nod+ / Fix-	Nod+ / Fix+	pNod	Nod+ / Fix+	Nod+ / Fix+	Nod+ / Fix+
CI-14A	Nod+ / Fix+	Nod+ / Fix-	Nod+ / Fix+	n.t.	n.t.	Nod+ / Fix+	Nod+ / Fix+
CI-19D	Nod+ / Fix+	Nod+ / Fix-	Nod+ / Fix+	n.t.	n.t.	Nod+ / Fix+	Nod+ / Fix+
CI-41S	Nod+ / Fix+	Nod+ / Fix-	Nod+ / Fix^{red}	pNod	Nod+ / Fix+	Nod+ / Fix^{red}	Nod+ / Fix^{red}
USDA 76^T	Nod+ / Fix+	Nod+ / Fix+	Nod+ / Fix+	n.t.	n.t.	Nod± / Fix^{red}	Nod+ / Fix+
NGR234	Nod+ / Fix+	Nod-	Nod+ / Fix+	Nod+ / Fix+	Nod+ / Fix+	Nod+ / Fix+	Nod+ / Fix+

Legend to Table S7. The following legumes were tested for nodulation: Cc, *Cajanus cajan* cv. ILRI 16555; Gm, *Glycine max* cv. Davis; Ma, *Macroptilium atropurpureum* cv. Siratro; Ll, *Leucaena leucocephala*; Tv, *Tephrosia vogelii*; Vr, *Vigna radiata* cv. King; Vu, *Vigna unguiculata* cv. Red Caloona. Nodulation assays were conducted in Magenta jars with two plants per pot, and with a fixed inoculum of 2 x 10^8 bacteria in 200 µl of sterile water per seedling. When needed, plants were watered using B&D nitrogen-free solution. Depending on the host, plants were grown for 35 to 98 days post-inoculation (dpi) before being harvested to assess the symbiotic phenotype of inoculated strains. Capacity of isolates to nodulate was scored as Nod+ for those forming nodules on all inoculated roots, Nod± for sporadic nodules formation, and pNod for strains that made only pseudonodules. Symbiotic nitrogen fixation was scored as strains being capable of sustaining harmonious plant growth (Fix+), poor plant development (Fix^{red}) or no growth beyond seed reserves (Fix-). As positive controls for nodulation and symbiotic nitrogen fixation, control plants were inoculated with strains *Bradyrhizobium elkanii* USDA 76^T or *Sinorhizobium fredii* NGR234. Some plant/strain combinations were not tested (n.t.).

Figure S1. Maximum likelihood phylogram inferred from partial 16S rRNA gene sequences.

The unrooted maximum-likelihood phylogram was inferred from partial 16S rDNA sequences of 57 type strains of the *Bradyrhizobium* genus, of *B. ivorense* sp. nov. strains CI-1B^T and CI-41S (shown in bold) and of *Methylobacterium nodulans* strain ORS 2060^T that was used as the outgroup. Sequences were aligned with MAFFT version 7 using Q-INS-i. The T92+G+I model was used with 1,184 positions and 1,000 pseudoreplicates as parameters. Only bootstrap values >70% are shown at branch nodes. Scale bar indicates the number of substitutions per site.

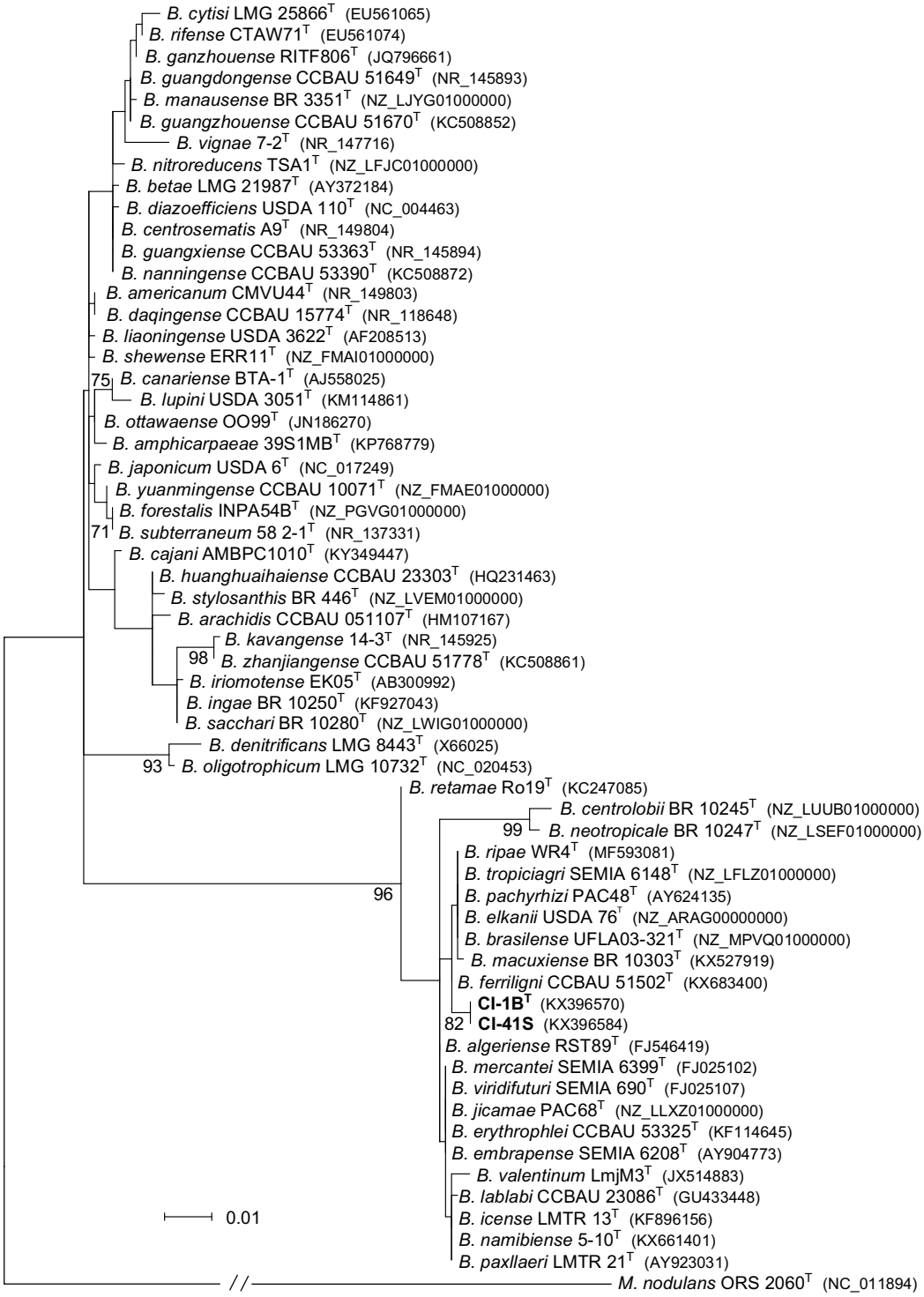

Figure S2. Maximum likelihood phylogram inferred from partial *dnaK* gene sequences.

The unrooted maximum-likelihood phylogram was inferred from 279 bp *dnaK* sequences of type strains of all species included in the *Bradyrhizobium elkanii* supergroup at the time of submission, of a selected number of additional *Bradyrhizobium* species, of *B. ivorense* sp. nov. strains CI-1B^T and CI-41S (shown in bold) and of *Methylobacterium nodulans* strain ORS 2060^T that was used as the outgroup. The TN93+G model was used with 279 positions and 1,000 pseudoreplicates as parameters. Only bootstrap values >70% are shown at branch nodes. Scale bar indicates the number of substitutions per site.

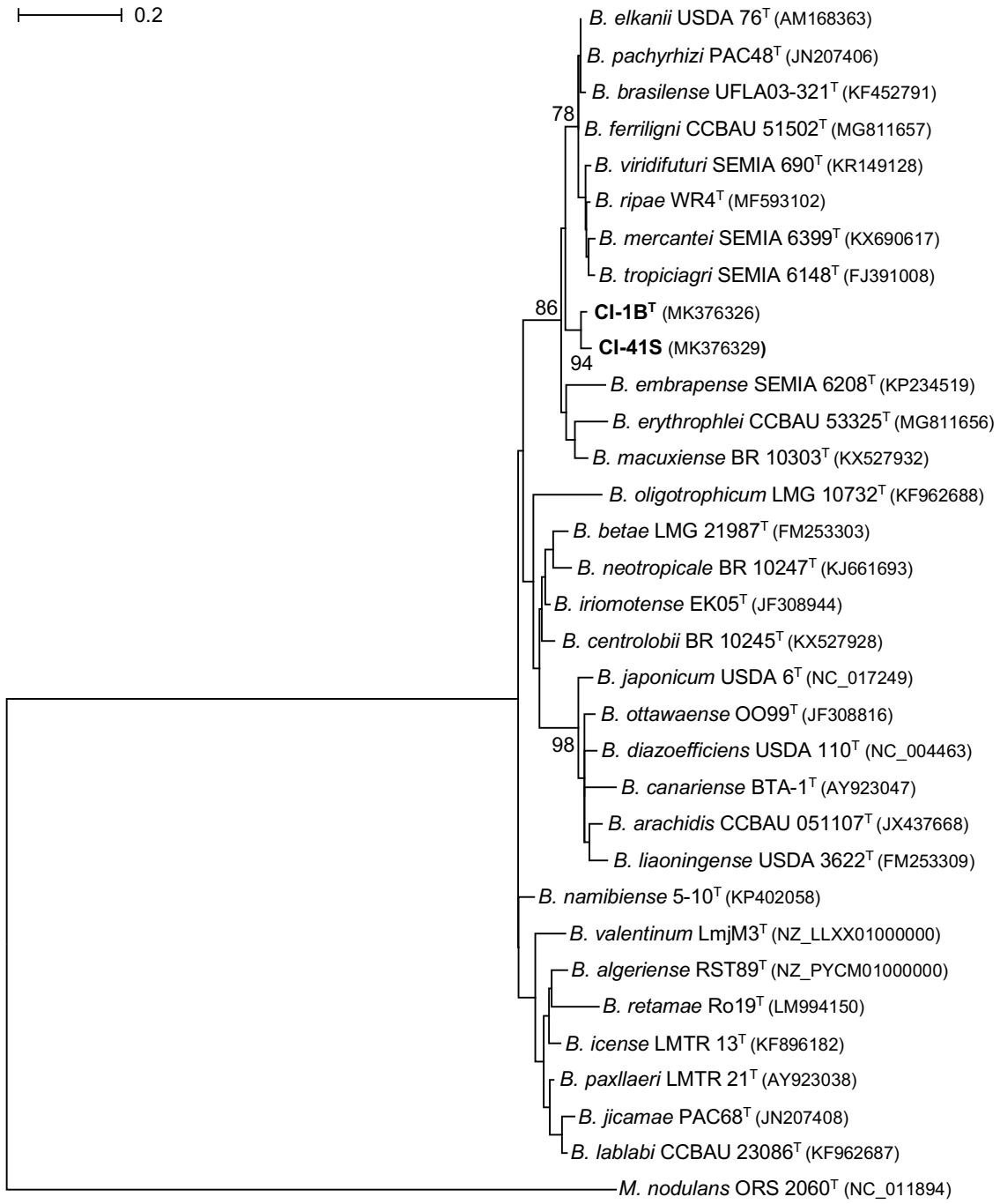

Figure S3. Maximum likelihood phylogram inferred from partial *glnII* gene sequences.

The unrooted maximum-likelihood phylogram was inferred from 540 bp *glnII* sequences of type strains of all species included in the *Bradyrhizobium elkanii* supergroup at the time of submission, of a selected number of additional *Bradyrhizobium* species, of *B. ivorense* sp. nov. strains CI-1B^T and CI-41S (shown in bold) and of *Methylobacterium nodulans* strain ORS 2060^T that was used as the outgroup. The GTR+G+I model was used with 540 positions and 1,000 pseudoreplicates as parameters. Only bootstrap values >70% are shown at branch nodes. Scale bar indicates the number of substitutions per site.

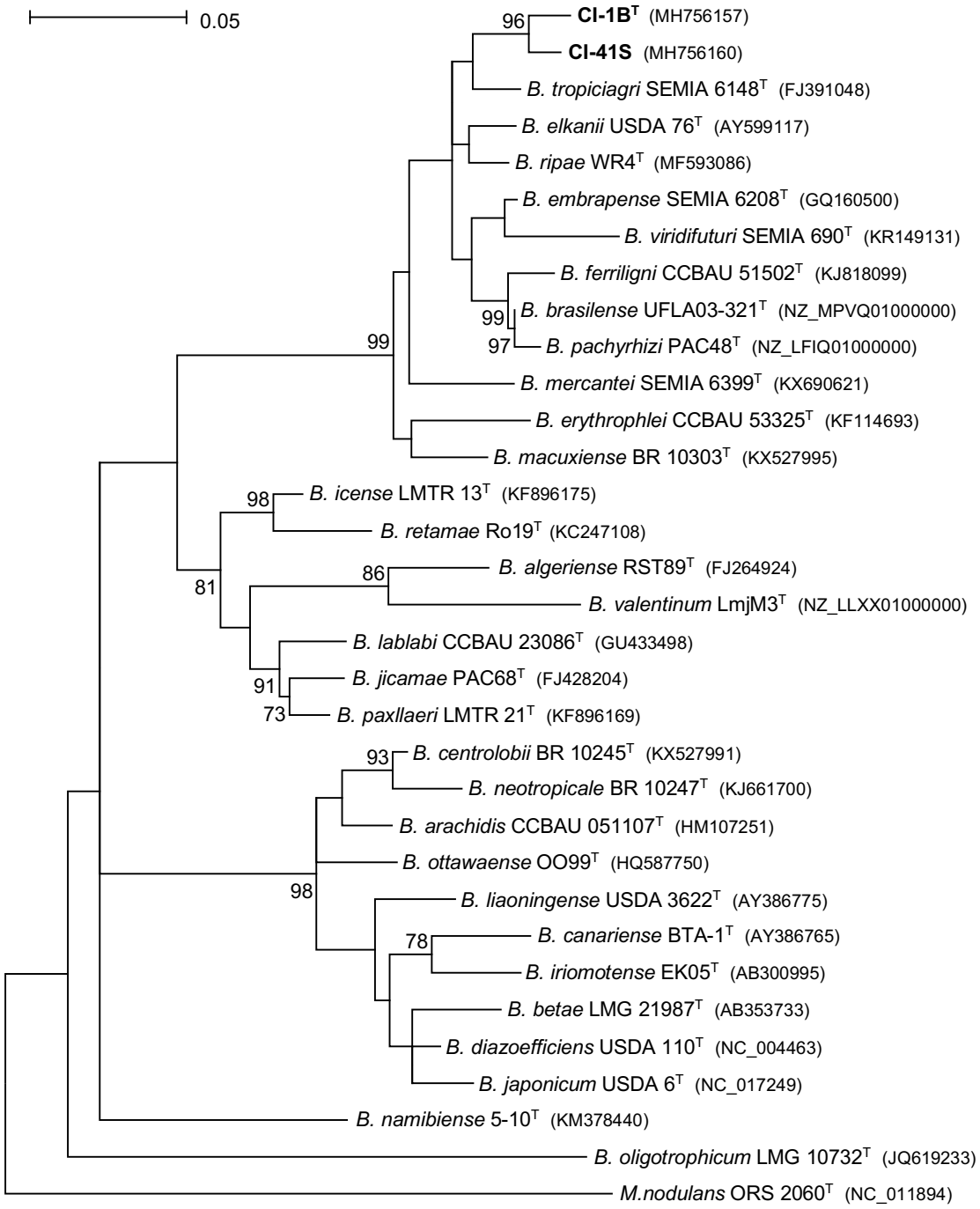

Figure S4. Maximum likelihood phylogram inferred from partial *gyrB* gene sequences.

The unrooted maximum-likelihood phylogram was inferred from 588 bp *gyrB* sequences of type strains of all species included in the *Bradyrhizobium elkanii* supergroup at the time of submission, of a selected number of additional *Bradyrhizobium* species, of *B. ivorense* sp. nov. strains CI-1B^T and CI-41S (shown in bold) and of *Methylobacterium nodulans* strain ORS 2060^T that was used as the outgroup. The T92+G model was used with 594 positions and 1,000 pseudoreplicates as parameters. Only bootstrap values >70% are shown at branch nodes. Scale bar indicates the number of substitutions per site.

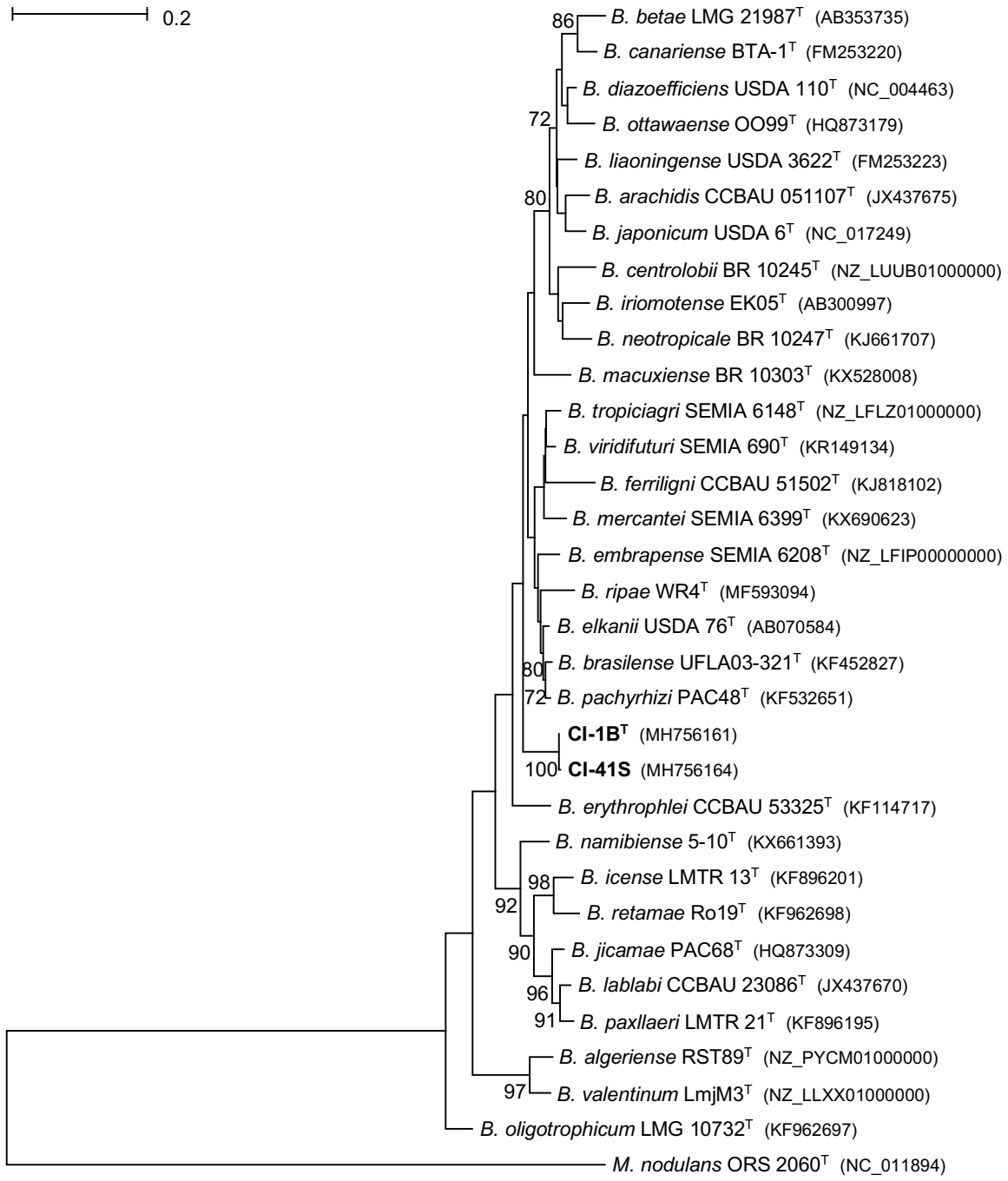

Figure S5. Maximum likelihood phylogram inferred from partial *recA* gene sequences.

The unrooted maximum-likelihood phylogram was inferred from 439 bp *recA* sequences of type strains of all species included in the *Bradyrhizobium elkanii* supergroup at the time of submission, of a selected number of additional *Bradyrhizobium* species, of *B. ivorense* sp. nov. strains CI-1B^T and CI-41S (shown in bold) and of *Methylobacterium nodulans* strain ORS 2060^T that was used as the outgroup. The T92+G model was used with 439 positions and 1,000 pseudoreplicates as parameters. Only bootstrap values >70% are shown at branch nodes. Scale bar indicates the number of substitutions per site.

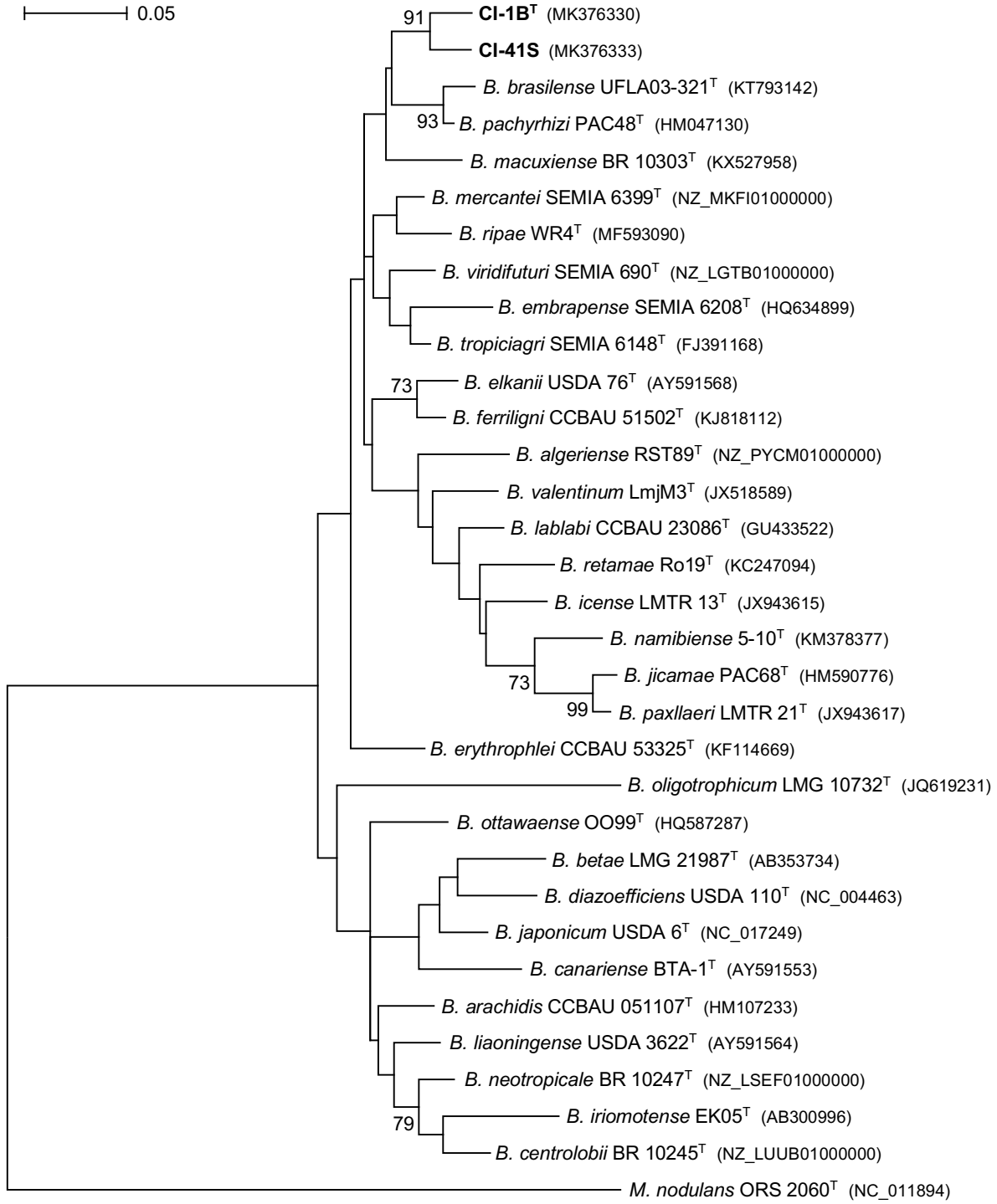

Figure S6. Maximum likelihood phylogram inferred from partial *rpoB* gene sequences.

The unrooted maximum-likelihood phylogram was inferred from 714 bp *rpoB* sequences of type strains of all species included in the *Bradyrhizobium elkanii* supergroup at the time of submission, of a selected number of additional *Bradyrhizobium* species, of *B. ivorense* sp. nov. strains CI-1B^T and CI-41S (shown in bold) and of *Methylobacterium nodulans* strain ORS 2060^T that was used as the outgroup. The GTR+G+I model was used with 714 positions and 1,000 pseudoreplicates as parameters. Only bootstrap values >70% are shown at branch nodes. Scale bar indicates the number of substitutions per site.

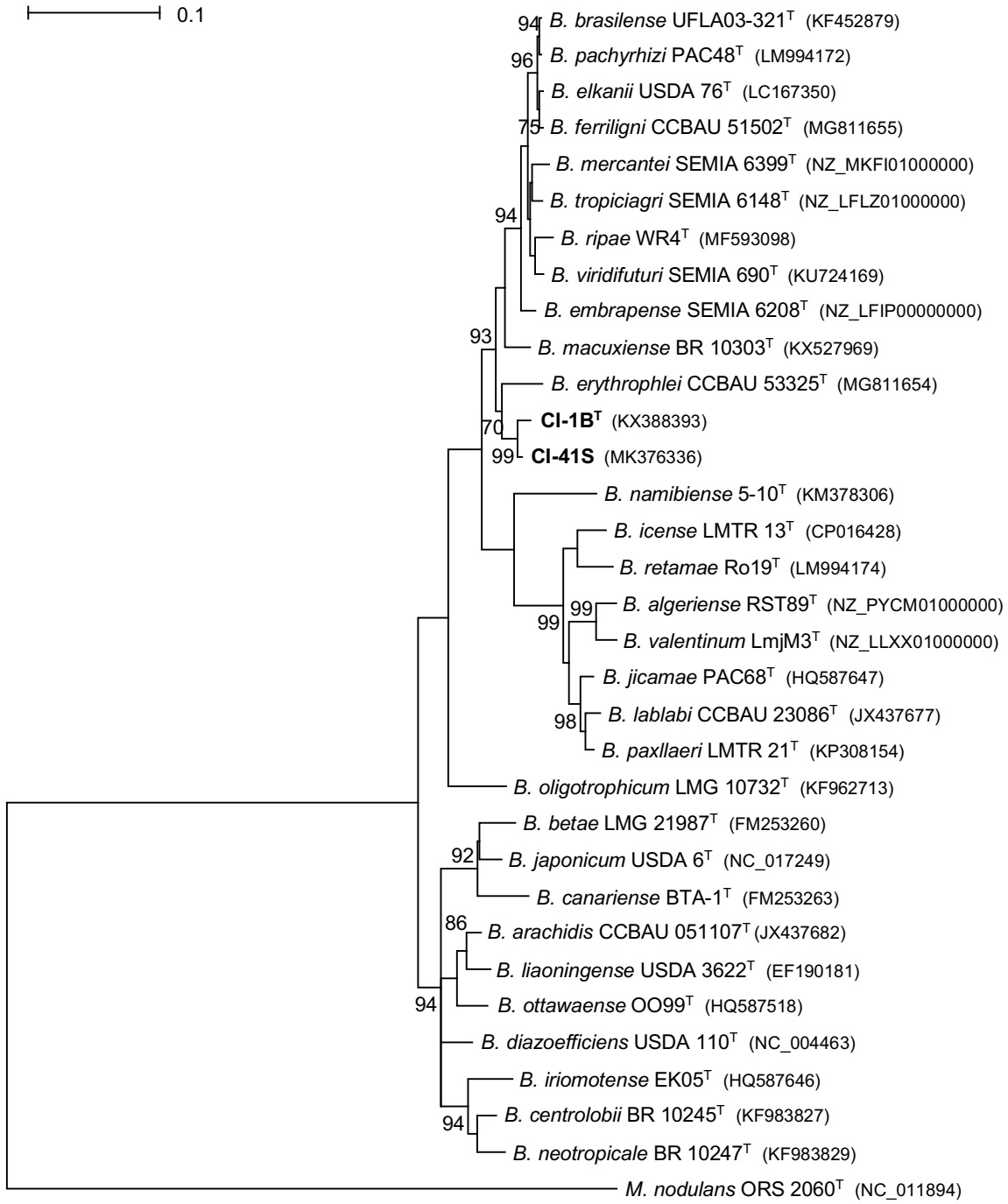

Figure S7. Maximum likelihood phylogram inferred from concatenated *glnII-recA* sequences.

The unrooted maximum-likelihood phylogram was inferred from concatenated partial *glnII* (522 bp) and *recA* (411 bp) sequences of 57 type strains of the *Bradyrhizobium* genus, of *B. ivorense* sp. nov. strains CI-1B^T and CI-41S (shown in bold) and of *Methylobacterium nodulans* strain ORS 2060^T that was used as the outgroup. The GTR+G+I model was used with 933 positions and 1,000 pseudoreplicates as parameters. Only bootstrap values >70% are shown at branch nodes. Scale bar indicates the number of substitutions per site.

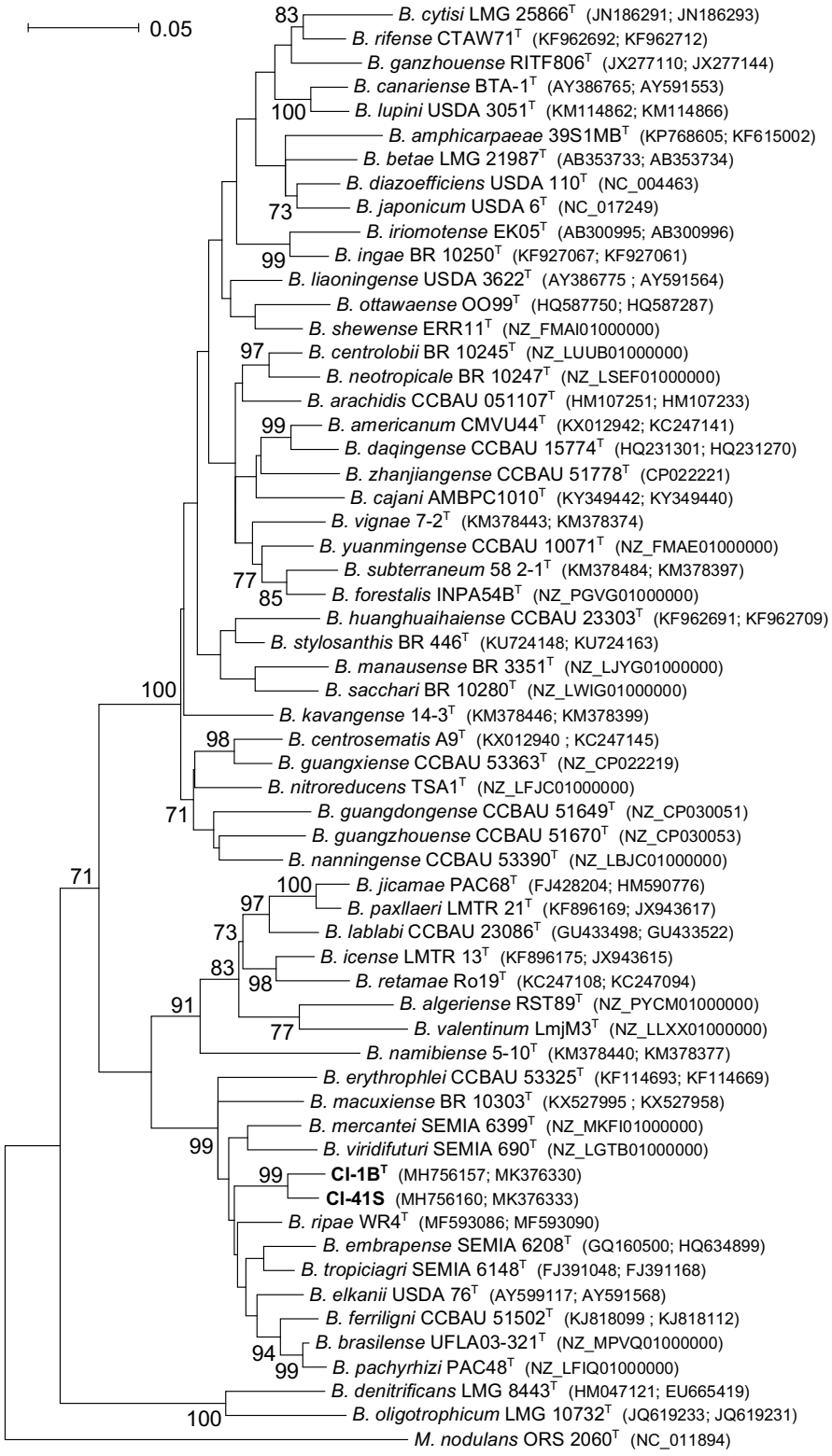

Figure S8. Maximum likelihood phylogram inferred from partial *nifH* gene sequences.

The rooted maximum-likelihood phylogram was inferred from 285 bp *nifH* sequences of type strains of all species included in the *Bradyrhizobium elkanii* supergroup at the time of submission, of a selected number of additional *Bradyrhizobium* species, of *B. ivorense* sp. nov. strains CI-1B^T and CI-41S (shown in bold) and of *Methylobacterium nodulans* strain ORS 2060^T that was used as the outgroup. The T92+G model was used with 285 positions and 1,000 pseudoreplicates as parameters. Only bootstrap values >70% are shown at branch nodes. Scale bar indicates the number of substitutions per site. Genomes of *B. centrolobii* BR 10245^T, *B. neotropicale* BR 10247^T and *B. oligotrophicum* LMG 10732^T were found to code for two divergent copies of *nifH*, both of which were included in this phylogeny. No *nifH* record was found for *B. betae* LMG 21987^T, *B. liaoningense* USDA 3622^T and *B. ripae* WR4^T strains that were included in other gene phylogenies, however.